

Influence of the surrounding host in obtaining tunable and strong visible photoluminescence from silicon nanoparticles

G. Santana, B. M. Monroy, A. Ortiz, L. Huerta, and J. C. Alonso^{a)}

Instituto de Investigaciones en Materiales, UNAM, Cd. Universitaria, A.P. 70-360, Coyoacán 04510, D.F. México

J. Fandiño

Instituto de Física, UNAM, Cd. Universitaria, A.P. 70-360, Coyoacán 04510, D.F. México

J. Aguilar-Hernández, E. Hoyos, F. Cruz-Gandarilla, and G. Contreras-Puentes

Escuela Superior de Física y Matemáticas del IPN; Edificio 9, U.P.A.L.M., 07738, D.F. México

(Received 22 August 2005; accepted 6 December 2005; published online 26 January 2006)

We have investigated the influence of the microstructure and chemistry of the surrounding host on the strong visible photoluminescence (PL) from silicon nanoclusters (nc-Si) embedded in three different silicon-based dielectric compounds: $\text{Si}_x\text{N}_y\text{:H,Cl}$, $\text{Si}_x\text{N}_y\text{O}_z\text{:H,Cl}$, and $\text{Si}_x\text{O}_z\text{:H,Cl}$, obtained from silicon nitride films deposited by $\text{SiH}_2\text{Cl}_2/\text{NH}_3/\text{H}_2$ plasma-enhanced chemical vapor deposition at different growth pressures. A blueshift is found in the PL coming from the nc-Si as the content of oxygen in the surrounding host is increased, and a significant improvement in PL intensity is achieved when the nc-Si are well passivated with O instead of H. We discuss the PL behavior in terms of the quantum confinement model and passivation state of the nc-Si surface.

© 2006 American Institute of Physics. [DOI: 10.1063/1.2164919]

The study of light emission from porous silicon and/or nc-Si embedded in different dielectric silicon compounds is important for producing low-cost integrated optoelectronic devices.^{1,2} The origin of such luminescence is often associated to quantum confinement effects in which the position of the photoluminescence (PL) energy peak depends fundamentally on silicon nanocluster (nc-Si) size.^{3,4} Several recent works have shown that the surface passivation of the nc-Si plays a crucial role, not only in reducing nonradiative processes and thus enhancing PL efficiency, but also in improving the emission stability.⁵⁻⁸ In spite of this, there are still many controversies on the importance and influence of the nc-Si surface chemistry and the different bonded passivants (hydrogen, nitrogen, oxygen, etc.) on the improvement of the PL.

Here we report the strong visible photoluminescence of nc-Si embedded in different silicon-based dielectric compounds obtained from silicon nitride films deposited by $\text{SiH}_2\text{Cl}_2/\text{NH}_3/\text{H}_2$ plasma-enhanced chemical vapor deposition (PECVD) at three different growth pressures (0.2, 0.5, and 1.0 Torr). We also discuss the influence of the nc-Si surface chemistry and/or bonded passivants on the photoluminescence behavior.

The films were deposited on high-resistivity, *n*-type, $\langle 100 \rangle$, monocrystalline silicon substrates, using a conventional PECVD system whose characteristics are reported elsewhere.⁹ Before deposition, the 1×1 cm silicon slices were etched in diluted hydrofluoric acid (5% HF) for removing the surface native oxide. High-purity Ar, SiH_2Cl_2 , NH_3 , and H_2 were used as precursor gases. The substrate temperature and the rf power were kept constant at 300 °C and 10 W, respectively. The flow rate ratio of $[\text{NH}_3]/[\text{SiH}_2\text{Cl}_2]$ was 1, while the hydrogen flow rate was of 40 sccm. Three

different types of films were obtained, depending on the deposition pressure (see Table I). The deposition time was adjusted for obtaining films with thickness around 1000 nm. After deposition, pieces of each sample were annealed in nitrogen for 1 h at a temperature of 1000 °C. A Gaertner L117 Ellipsometer equipped with a He-Ne laser ($\lambda = 632.8$ nm) was used to measure the refractive index and thickness of the films. The chemical bonding behavior was analyzed by means of a Fourier transform infrared (FTIR) spectrophotometer (Nicolet-210). X-ray photoelectron spectroscopy (XPS) analysis of the composition was performed with the aid of a VG Microtech Multilab ESCA 2000 system. The scanning electron microscopy (SEM) images were obtained with a XL 30 FEG/SIRION with focused ion- and electron-beam, energy dispersive x-ray spectroscopy, and energy dispersive angle x-ray GENESIS 4000. Photoluminescence studies were carried out at room temperature in a conventional PL system described in detail elsewhere.¹⁰ A 10 mW He-Cd laser (325 nm) was used as excitation source. All the spectra were corrected taking into account the spectral response of the system.

The array of SEM images in Fig. 1 shows that film A is dense and homogeneous; meanwhile, films B and C are inhomogeneous and porous (formed by a mixture of a solid

TABLE I. Deposition rate (DR), refractive index (*n*) and relative composition of as grown (A,B,C) and annealed (Aa, Ba, Ca) silicon nitride films deposited by PECVD at different pressures (*P*).

Sample	<i>P</i> (torr)	DR (nm/min)	<i>n</i>	N/Si	O/Si	Cl/Si
A	0.2	9.6	2.03	0.54	0.038	0.25
Aa	0.2	...	1.99	0.54	0.045	0.23
B	0.5	16.8	1.79	0.13	1.58	0.05
Ba	0.5	...	1.68	0.12	1.59	0
C	1.0	29.4	1.29	0.08	1.85	0.03
Ca	1.0	...	1.27	0.05	1.7	0

^{a)} Author to whom correspondence should be addressed; electronic mail: alonso@servidor.unam.mx

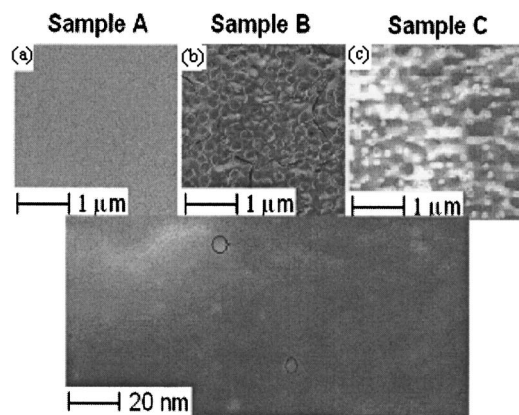


FIG. 1. SEM images showing the surface morphology of samples A, B, and C. The inferior SEM image is a cross section view of one of the samples, where the roughness and silicon nanoclusters are shown.

phase and voids). As it is shown in the high-resolution SEM image at the bottom of Fig. 1, all the films consisted of nanometric particles (nc-Si) embedded in an amorphous matrix (surrounding host). According to the XPS composition data shown in Table I, and the features of the IR spectra shown in Fig. 2, the compositions of films A, B, and C, correspond mainly to hydrogenated-chlorinated silicon nitride film ($\text{SiN}_x\text{:H,Cl}$), hydrogenated-chlorinated silicon oxynitride film ($\text{SiO}_x\text{N}_y\text{:H}$), and hydrogenated porous silicon oxide ($\text{SiO}_x\text{:H}$), respectively. All these compounds are silicon rich. The refractive indexes of samples A, B, and C, which are 2.03, 1.79, and 1.29, respectively, correspond with the shift in the composition of the films from silicon nitride to silicon oxide. The low refractive index of sample C (lower than 1.46), in spite of its silicon-rich composition, confirms

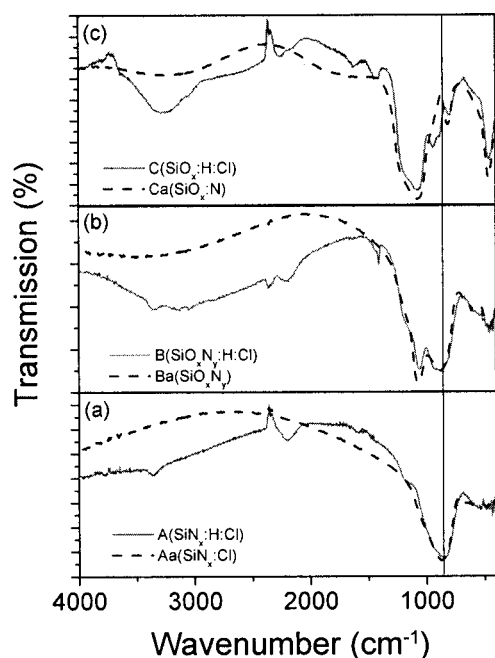


FIG. 2. FTIR spectra of as-grown and annealed samples: (a) A and Aa, (b) B and Ba, and (c) C and Ca. The assignment of bands is the following: Si—N stretching ($\sim 855\text{ cm}^{-1}$), N—H stretching and rocking (~ 3350 and 1185 cm^{-1}), N—H₂ bending and stretching (~ 1400 and 3050 cm^{-1}), Si—H stretching ($\sim 2200\text{ cm}^{-1}$), Si—O stretching, bending, and rocking (~ 1070 , 810 , and 445 cm^{-1} , respectively), Si—OH bonds and/or adsorbed H₂O (940 cm^{-1} and $3000\text{--}3600\text{ cm}^{-1}$, respectively), Si—Cl bonds (450 to 625 cm^{-1}) (See Refs. 9, 14, and 15).

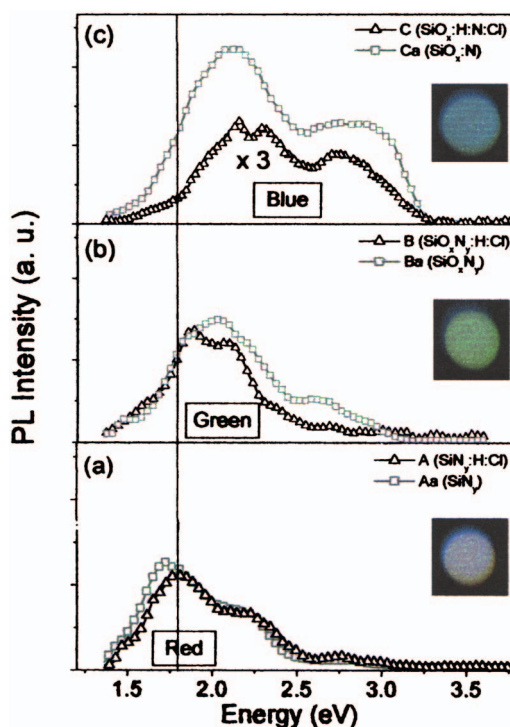


FIG. 3. Room-temperature PL spectra of as-grown and annealed samples: (a) A and Aa, (b) B and Ba, and (c) C and Ca. The insets show the corresponding emission color of the PL spot, as they are seen with the naked eye.

that this film is very porous. The partial and total oxidation of films B and C, respectively, can be understood as a result of their high porosity, which in turn is a consequence of their high deposition rate, which also means a high incorporation of SiCl_x radicals. Films with high Cl content tend to be porous and prone to suffer a fast and complex hydrolyzation/oxidation process when they are exposed to the ambient moisture, in which chlorine is removed from the films and substituted by O and H atoms.^{11–14} This explanation is consistent with the fact that the chlorine content in the as-deposited films A, B, and C is inversely proportional to the oxygen content (see Table I).

The use of SiCl_2H_2 in the PECVD process also favors the formation of clusters with nanometric size within the growing film.^{11–13} The formation of the nc-Si is understood as a result of a combination between the release of disorder induced stress and enhanced chemical reactivity of SiHCl -related complex, created by the impinging atomic hydrogen, which promote the phase transition from amorphous to nanocrystalline silicon under adequate conditions.^{11,12}

According to our compositional and structural results, our nc-Si are surrounded by N, O, Cl, and H atoms, in different relative amounts, which depend on film porosity, reactivity with the ambient moisture, and the annealing process.

The PL coming from the nc-Si surrounded by the different dielectric hosts was in the range from 1.5 to 3.0 eV, and for most of the samples was strong enough to be observed with the naked eye in a bright room. As Fig. 3 shows, the overall color of the emission of the as-deposited samples is bluishifted as the oxygen content in the surrounding host of the nc-Si increased. The positions of the maximum PL are around 1.80, 1.94, and 2.15 eV for samples A, B, and C, respectively. Thus, according to the quantum confinement model,³ the average sizes (a , in nanometers) of the nc-Si (quantum dots) calculated using the formula $E\text{ (eV)}=1.16$

+11.8/ a^2 , where E is the PL energy peak, were approximately, 4.29, 3.86, and 3.45 nm, respectively. The reduction in the size of the nc-Si embedded in the matrix of samples B and C, compared with that of sample A, can be explained assuming that the oxidation of samples B and C, consumes Si atoms from the surface of the nc-Si.¹³ The strong luminescence of the as-deposited samples A and B, indicates that the nc-Si are well passivated, mainly by N, Cl, and H in the first case, and O and H in the second case. The low total PL intensity of the as-deposited sample C indicates that in this case the host matrix does not provide good passivation of the surface of the nc-Si. This poor passivation is very probably due to the existence of many dangling bonds on the nc-Si surface which function as nonradiative recombination centers, generated by the high porosity of this sample, and/or the large stress at the Si/SiO₂ interface of the nc-Si.

The disappearance of the absorptions bands related to Si–H and N–H bonds in the IR spectra (dotted lines of Fig. 2) of the annealed samples (Aa, Ba, and Ca) along with the corresponding composition data of Table I, show that the main effect of the annealing process on the composition of all the samples is the total loss of hydrogen. This means that all the H atoms providing passivation of the nc-Si surface in the as deposited films have been substituted, mainly by N and/or O atoms in the annealed samples. The marginal changes observed in PL spectra of samples A and B, with the annealing process, indicates that for these samples the change of the nc-Si passivant H atoms, by N in the first case and O in the second case, does not have an important influence on their PL characteristics. The small redshift observed in the PL spectrum of sample Aa with respect to that of sample A, can be due to the substitution of Si–H bonds by Si–Si bonds at the nc-Si surface during annealing, which has the effect of increasing the nc-Si size and/or surface reconstruction. The small blueshift found in the PL spectrum of the annealed sample Ba with respect to that without annealing (B), can be due to the further reoxidation of nc-Si when it enters in contact with air again after annealing, which, as it was mentioned before, should reduce the nc-Si size.

For the annealed sample Ca, the radiative efficiency is considerably enhanced with a noticeable shift towards higher energies and widening of the PL spectrum. This effect is believed to be caused by the reorganization of the structure and bonding configuration of the whole host matrix and nc-Si surface, which leaves nc-Si with a surface very well passivated with only O atoms. The blueshift as well as the increase in PL peak intensity are probably originated by the formation of new small silicon nanoclusters in the films. Because the diffusivity of the Si atoms in the silicon oxynitride

and silicon oxide matrices is rather low, the Si atoms might diffuse only a short distance creating additional small Si clusters. The diffusion process also favors the size enlargement of the Si clusters that already exist, originating a redshift in the PL. Both effects, redshift and blueshift, generated as a consequence of this transformation produce the widening of the PL spectrum of sample Ca.

In conclusion, our results show that the PL of the nc-Si depends not only on their size and density, but also on the state and nature of their surface passivation provided by the surrounding host. According to the quantum confinement model, the blueshift found in the PL coming from the nc-Si as the content of oxygen in the surrounding host is increased, can be explained in terms of a reduction in the nc-Si average size as a consequence of their oxydation. The changes observed in the PL characteristics of the annealed samples with respect to the as deposited ones show that the substitution of H as passivant of the nc-Si surface by N has small effects on the PL efficiency, but the passivation with O produces a significant enhancement in this efficiency.

The authors acknowledge the technical assistance of J. Camacho, S. Jimenez, M.A. Canseco, and partial financial support for this work from CONACyT-México under project 47303-F and PAPIIT-UNAM under project IN-109803.

¹B. H. Kim, C. H. Cho, T. W. Kim, N. M. Park, G. Y. Sung, and S. J. Park, *Appl. Phys. Lett.* **86**, 091908 (2005).

²L. Y. Chen, W. H. Chen, Kim, and F. C. N Hong, *Appl. Phys. Lett.* **86**, 193506 (2005).

³T. Y. Kim, N. M. Park, K. H. Kim, and G. Y. Sung, Y. W. Ok, T. Y. Seong, and C. J. Choi, *Appl. Phys. Lett.* **85**, 5355 (2004).

⁴N. M. Park, C. J. Choi, T. Y. Seong, and S. J. Park, *Phys. Rev. Lett.* **86**, 1355 (2001).

⁵E. W. Draeger, J. C. Grossman, A. J. Williamson, and G. Galli, *Phys. Rev. Lett.* **90**, 167402 (2003).

⁶A. Puzder, A. J. Williamson, J. C. Grossman, and G. Galli, *Phys. Rev. Lett.* **88**, 097401 (2002).

⁷M. V. Wolkin, J. Jorne, P. M. Fauchet, G. Allan, and C. Delerue, *Phys. Rev. Lett.* **82**, 197 (1999).

⁸M. S. Yang, K. S. Cho, J. H. Jhe, S. Y. Seo, J. H. Shin, K. J. Kim, and D. W. Moon, *Appl. Phys. Lett.* **85**, 3408 (2004).

⁹G. Santana, J. Fandiño, A. Ortiz, and J. C. Alonso, *J. Non-Cryst. Solids* **351**, 922 (2005).

¹⁰J. Aguilar-Hernández, G. Contreras-Puente, J. M. Figueroa-Estrada, and O. Zelaya-Angel, *Jpn. J. Appl. Phys., Part 1* **33**, 37 (1994).

¹¹T. Ito, K. Hashimoto, and H. Shirai, *Jpn. J. Appl. Phys., Part 2* **42**, L1119 (2003).

¹²H. Liu, S. Jung, Y. Fujimura, H. Shirai, and Y. Toyoshima, *Jpn. J. Appl. Phys., Part 2* **40**, L215 (2001).

¹³H. Shirai, T. Tsukamoto, and K. I. Kurosaki, *Physica E (Amsterdam)* **16**, 388 (2003).

¹⁴J. C. Alonso, R. Vazquez, A. Ortiz, V. Pamkov, and E. Andrade, *J. Vac. Sci. Technol. A* **16**, 3211 (1998).

¹⁵G. Lucovsky and S. Y. Lin, *J. Vac. Sci. Technol. B* **3**, 1122 (1985).